Paper No. 1315. (quote when citing this article)
Eleventh World Conference on Earthquake Engineering
ISBN: 0 08 042822 3

BRIDGE ABUTMENT STIFFNESS DURING EARTHQUAKES

RAKESH K. GOEL
Department of Civil and Environmental Engineering
Syracuse University, Syracuse, NY 13244-1190.

ABSTRACT

The 'actual' stiffness values of the abutment-soil systems at the US 101/Painter Street Overpass are determined from the ground and structural motions recorded during earthquakes using a simple equilibrium-based approach without finite-element modeling of the structure or of the abutment-soil systems. These values of the abutment stiffness, which include the effects of soil-structure interaction and nonlinear behavior of the soil, are used to (1) investigate the effects of abutment deformation on the abutment stiffness and (2) evaluate the CALTRANS, AASHTO-83, and ATC-6 procedures for estimating the abutment stiffness. Presented results show that the 'actual' abutment stiffness may be significantly different during different phases of the shaking and decreases significantly as the abutment deformation increases. Evaluation of the current procedures shows that the CALTRANS procedure leads to a good estimate of the abutment stiffness in the direction along the abutment (transverse to the deck) provided the deformation assumed in computing the stiffness is close to the actual deformation during an earthquake. However, this procedure may overestimate the stiffness normal to the abutment (along the road deck) by a factor of over two indicating that the assumed value of 7.7 ksf for the ultimate passive resistance of the soil, which is used in the CALTRANS procedure, may be too high. The AASHTO-83 and ATC-6 procedures lead to an initial estimate of the abutment stiffness that is too high in both directions.

KEYWORDS

Abutment stiffness; abutment-soil system; bridge abutments; bridge codes; bridge design; earthquake design; seismic design.

INTRODUCTION

Most specifications and guidelines for earthquake design of highway bridges require that abutment-soil systems be included in the analytical model as discrete equivalent linear springs (CALTRANS, 1988 and 1989; ATC-6, 1981; AASHTO-83, 1988). In design applications, stiffness values of these springs are usually determined either based on simplified rules and an iterative process, or from abutment capacity and expected deformation during the earthquake. It is not entirely clear how well the stiffness value thus determined represents the complex behavior of the abutment-soil system, which is influenced by soil-

structure interaction and nonlinear behavior of the soil. Therefore, it would be useful to compare the 'design' values of abutment-soil stiffness with their 'actual' values during earthquakes.

In this investigation, the 'actual' values stiffness of the abutment-soil systems at the US 101/Painter Street Overpass are determined from the ground and structural motions recorded during earthquakes. These values are estimated from the force-deformation relations for the abutment-soil systems determined from the recorded motions using the dynamic equilibrium of the road deck. The abutment stiffness thus obtained include all effects, including those of soil-structure interaction and nonlinear behavior of the soil. These results are used to (1) investigate the effects of abutment deformation on the abutment stiffness and (2) evaluate the CALTRANS, AASHTO-83, and ATC-6 procedures for estimating the abutment stiffness.

STRUCTURE AND RECORDED MOTIONS

The structure considered in this study is the US 101/Painter Street Overpass (Figure 1) located in Rio Dell, California. This 265 ft long bridge consists of a continuous reinforced-concrete (R/C) multi-cell box-girder road deck supported on integral abutments at the two ends and on an R/C two-column bent. The bent divides the bridge into two unequal spans of 119 ft and 146 ft. Both abutments and bent are skewed at an angle of 38.9°. The east abutment is monolithic with the superstructure and is supported on 14 driven 45-ton concrete friction piles. The west abutment rests on a neoprene bearing strip that is part of a designed thermal expansion joint of the road deck. The foundation of this abutment consists of 16 driven 45-ton concrete friction piles.

The US 101/Painter Street Overpass was instrumented by the California Strong Motion Instrumentation Program (CSMIP) in 1977. Figure 1 also shows locations of the sensors and identifies the 20 data channels. Motions of this overpass have been recorded during nine earthquakes, two of which have been selected here: the main shock of the April 25, 1992, Cape Mendocino/Petrolia earthquake and the second event of the November 21, 1986, Cape Mendocino earthquake. The first of these two earthquakes is an infrequent large event which may represent the design earthquake and the latter is a frequent small event which may represent the service level earthquake.

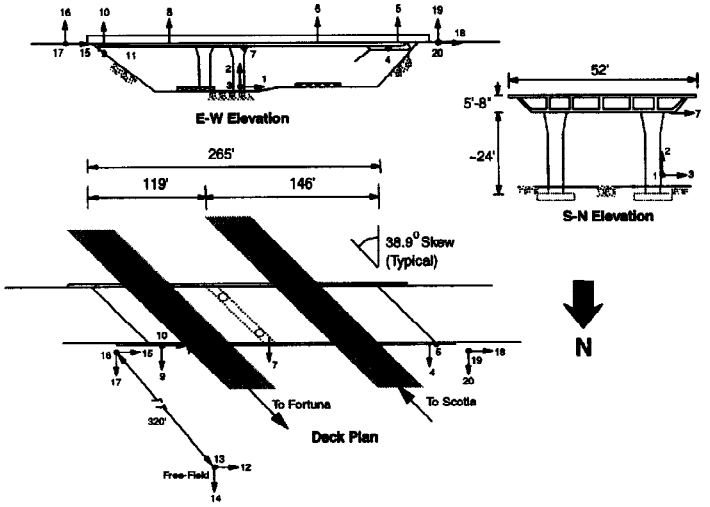

Figure 1. US 101/Painter Street Overpass: structural details and sensor locations.

ANALYSIS PROCEDURE

Structural Idealization

Figure 2 shows the free-body diagram of an idealized model of the US 101/Painter Street Overpass. The model consists of the road deck with three spring-damper systems, which represent the stiffness and

damping properties of abutment-soil systems along the east abutment, normal to the east abutment, and along the west abutment. The spring represents the stiffness property and the damper accounts for material and radiation damping of the abutment-soil system. Each column in the central bent is represented by two linear elastic springs -- one normal to and the other along the bent; no damper is included because the energy dissipation in the bent should be negligible. Each column in the bent is modeled explicitly to properly account for the contribution of the bent stiffness to the total torsional stiffness about the vertical axis of the overpass. Furthermore, the columns are assumed to be linearly elastic because no cracking was observed in the columns even after the strongest shaking during the April 25, 1992, Cape Mendocino/Petrolia earthquake.

Abutment Forces and Deformations

The abutment forces are computed by solving the three equations of dynamic equilibrium for the system in the x, y, and θ directions. For the system of Figure 2, all the forces except the resisting forces associated with the abutments are known. The inertia forces associated with the rigid-body motion of the road deck are computed from the mass properties of the deck and its recorded accelerations. The additional inertia forces due to the in-plane deformations of the road deck in the y-direction are included by assuming that the deformation over the length of the deck varies as a half-cycle of a sine function. Amplitude of the sine function is taken as in-plane deformation of the deck at its center of mass. The force in each column spring is calculated from its stiffness and deformation. The column stiffness in each of the two orthogonal directions is half of the bent stiffness along the respective direction. The stiffness along the bent is the lateral stiffness of a frame formed by the columns and the cap-beam. Similarly, stiffness normal to the bent is the lateral stiffness of a frame consisting of the columns and the road deck. In computing the frame stiffnesses, the moment of inertia of the column is selected as its cracked value in the moment curvature relationship and the moment of inertia values of the cap-beam and the box girder are obtained from their structural details.

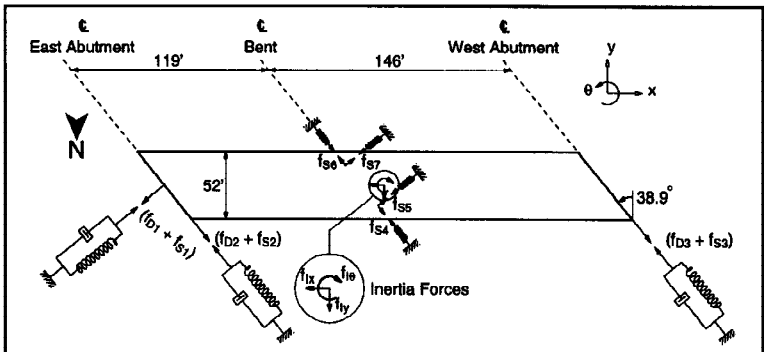

Figure 2. Free-body diagram for structural idealization of US 101/Painter Street Overpass.

At each time-instant the deformation in an abutment spring-damper system or a column spring is obtained by subtracting the free-field displacement from the displacement at the top of the abutment or the column, respectively. The displacements are obtained by appropriately transforming displacements at the sensor positions to the desired locations. Further details of the analysis procedure are available elsewhere (Goel and Chopra, 1994).

Abutment Stiffness

Solution of the aforementioned dynamic equilibrium equations at each time instant leads to the abutment forces which can be plotted against the computed deformations to obtain the force-deformation hysteresis loops. Figure 3 shows such loops for the three abutment springs during the 1992 earthquake. The stiffness of the abutment-soil system is determined by isolating individual loops (Figure 4) from the force-deformation hysteresis loops (Figure 3). The nearly elliptical shape of the loop representing the force-deformation relation normal to the east abutment (Figure 4a) suggests that the behavior was like linearly visco-elastic. The spring stiffness is the slope of the major axis of the ellipse; the two plausible axes shown in Figure 4a indicate stiffness values of 13,115 and 11,000 kips/ft. Unlike the previous loop, the loop shown in Figure 4b exhibits significant nonlinearity as evident from nearly the elasto-plastic behavior with strain hardening effects. From such loops, the upper and lower bounds of the stiffness can

be estimated from the secant slopes: 7500 and 12000 kips/ft for the positive and negative deformations, respectively.

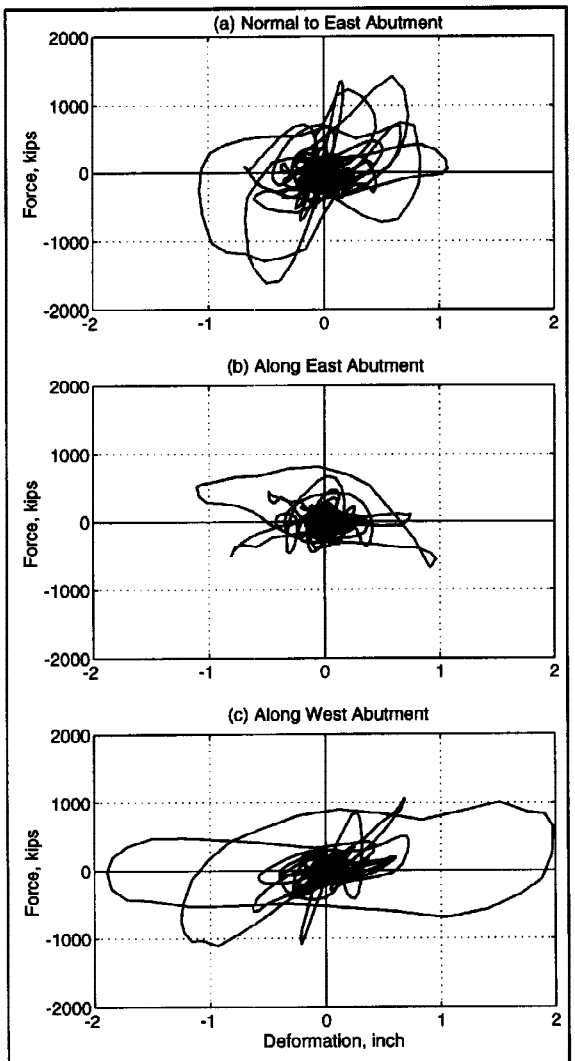

Figure 3. Abutment force-deformation relationships during the 1992 earthquake.

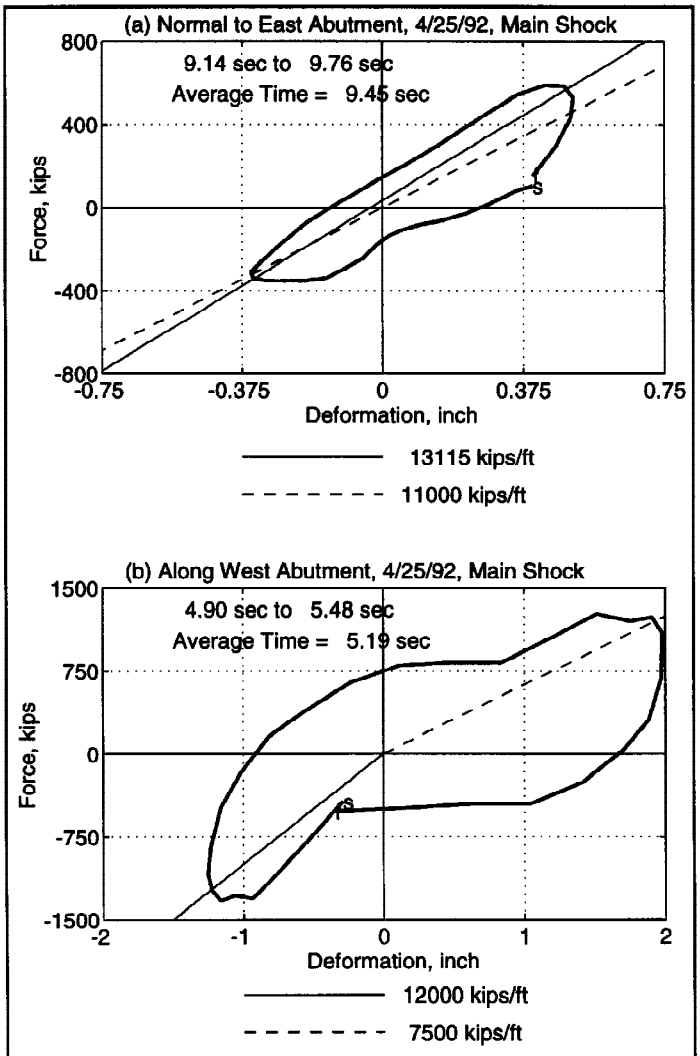

Figure 4. Estimation of abutment stiffness from the abutment force-deformation relationships.

EFFECTS OF ABUTMENT DEFORMATION ON ABUTMENT STIFFNESS

How the deformation of the abutment influences its stiffness is investigated next. The total deformation during a single hysteresis loop is defined as the sum of the deformation amplitudes in the positive and negative directions of the loop. Both stiffness and deformation of an abutment are determined from hysteresis loops at different time instants. Such properties during the intense shaking of the 1992 earthquake are presented and compared with those during the much smaller shaking of the 1986 earthquake.

Time-Variation of Abutment Deformation and Stiffness

Figure 5 shows the time-variation of the abutment stiffness (solid circles) with its scale on the left hand side and of the total deformation (open circles) with its scale on the right hand side; the upper and lower bound values of the stiffness are connected by a vertical line; the results presented are for the 1992 earthquake. These values determined from a hysteresis loop, as described in the preceding section, were plotted at the time instant when half of the loop had been completed. It is apparent from these results that

the abutment stiffness, which depends on the deformation, varies significantly during the same earthquake; this variation is particularly large for the stiffness normal to the east abutment (Figure 5a). In particular, these results show the following general trends:

- The abutment tends to be stiff for the small deformations during the build-up phase of the shaking.
- The abutment stiffness decreases as its deformation increases during stronger shaking.
- The abutment recovers some of its stiffness with subsequent reduction in its deformation as the motion becomes less intense towards the later part of the shaking.
- The stiffness recovery is only partial and gradual over time; the recovery is especially slow after repeated cycles of large deformation.

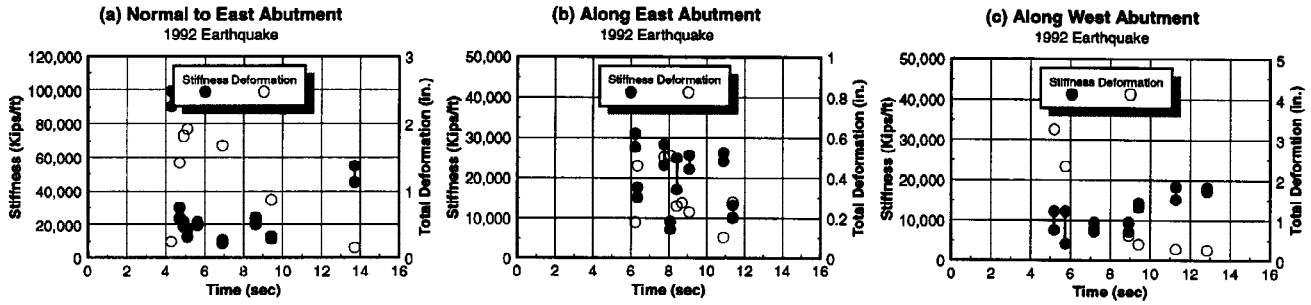

Figure 5. Time variation of abutment stiffness and deformation during the 1992 earthquake.

The above-noted trends during the build-up phase are more prominent for stiffness normal to the east abutment compared to stiffness along the east abutment and the stiffness along the west abutment. Such is the case because meaningful hsysteresis loops could not be isolated for the latter two abutments and their stiffness values were not identified. However, it is expected that the trends for all the stiffness values would be similar.

The above-identified behavior of abutments during earthquakes indicates that the soil enclosed between the wingwalls provides significant resistance to the abutment motion for small deformation levels, but becomes less effective at larger deformations. Some of the reduction in stiffness at large deformation is due to the nonlinear behavior of the abutment-soil system apparent from hysteresis loops of Figure 3.

Time-Variation of Abutment Stiffness During Two Earthquakes

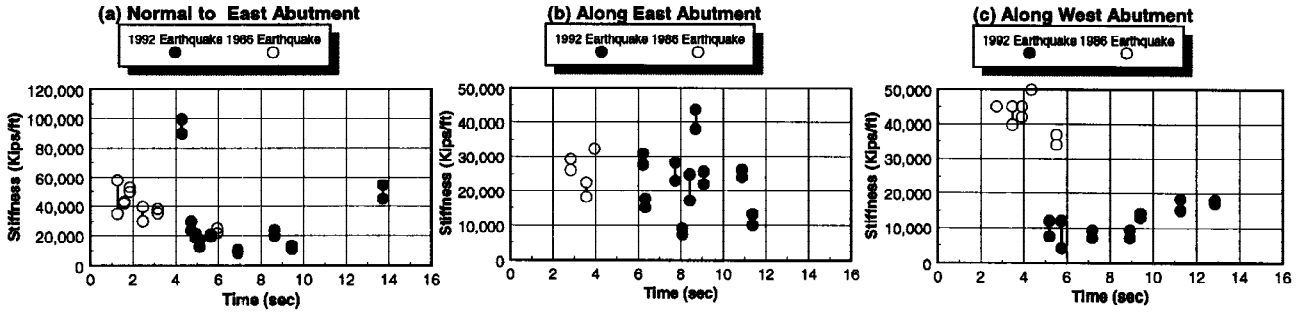

Figure 6. Time-variation of abutment stiffness during the 1992 and 1986 earthquakes.

The abutment stiffness values during the intense shaking of the 1992 earthquake and the much smaller motions of the 1986 earthquake are compared in Figure 6. These results show that the abutment behavior is consistent with the trends identified in the previous section. The abutment is generally less stiff during the 1992 earthquake (Figures 6a and 6c) because the abutment deformations are larger compared to the

1986 earthquake; the peak abutment deformations during the former earthquake are almost ten times those during the latter earthquake (Goel and Chopra, 1994). This reduction in stiffness is more pronounced for the west abutment because its deformations are larger due to torsional motions of the road deck during the 1992 earthquake. If the deformations during the two earthquakes are similar, as in the transverse direction at the east abutment, the abutment stiffnesses are also similar (Figure 6b).

EVALUATION OF CURRENT PROCEDURES

The 'design' values of the abutment capacity and abutment stiffness, computed by the CALTRANS, AASHTO-83, and ATC-6 procedures, are compared in this section with their 'actual' values obtained by the aforementioned procedure applied to the 1992 earthquake records. Described first are the current procedures to calculate the 'design' values followed by comparison of the 'design' and 'actual' values of the abutment stiffness.

Current Procedures

In the CALTRANS procedure, the 'design' value of the abutment stiffness is computed as the ratio of the abutment capacity and the acceptable deformation. In this investigation, two values of the acceptable abutment deformations are considered: 1 inch and 2.4 inch. The first represents the deformation at which the soil pressure reaches its peak value of 7.7 ksf and the latter represents the limiting value corresponding to incipient damage to the abutment (CALTRANS, 1988 and 1989).

The abutment capacity in the longitudinal direction is computed as sum of the resistance values provided by the foundation and the soil behind the backwall. It is assumed the backfill is mobilized to a depth equal to the depth of the superstructure and the ultimate passive resistance of the backfill is equal to 7.7 ksf (CALTRANS, 1989). Since the foundation capacity depends on which of its components fails first, its value is calculated for the following four cases: (1) diaphragm at the monolithic east abutment reaches its shear capacity; (2) piles at the east abutment reach their peak resistance values; (3) diaphragm at the east abutment reaches its shear capacity and the piles at the west abutment reach their peak resistance values; and (4) piles at the east and the west abutments reach their peak resistance values.

The first two cases correspond to resistance provided only by the foundation at one abutment before the expansion joint gap closes or after the longitudinal shear key at the west abutment fails, whereas the other two cases correspond to resistance provided by both the abutments when the shear key is engaged at the west abutment. The first and third cases assume shear failure in the backwall just below the road deck soffit before the piles fail, whereas the second and the fourth cases assume failure of piles before the backwall fails.

The abutment capacity in the transverse direction is computed as sum of the shear capacity of one wingwall and the foundation capacity. The foundation capacity for the monolithic east abutment is assumed equal to the peak resistance offered by the piles whereas that for the west abutment it is taken equal to the capacity of the transverse shear key. According to CALTRANS recommendations, the capacity of the shear key is computed as 0.75 times the peak resistance offered by the piles.

In the AASHTO-83 and ATC-6 procedures, which are identical, two estimates -- initial and final -- for the 'design' value of the abutment stiffness are calculated. The initial estimate of the abutment is obtained by adding the contributions of the backfill and of the piles (Lam and Martin, 1986). The stiffness due to the backfill is $0.425 \times E_s \times B$, in which $E_s = 1440$ ksf is the elastic modulus of the soil and B is the width of the backwall or effective length of the backwall or the wingwall. The stiffness of each pile is assumed equal to 40 kips/inch. The final stiffness value is obtained by an iterative procedure in which the abutment stiffness is successively reduced till the computed abutment force does not exceed the abutment capacity. Although, AASHTO-83/ATC-6 specifications mention that the abutment capacity may be computed from ultimate resistance values of the soil and the piles, guidelines for these computations are lacking. If the

abutment capacity is assumed equal to that by the CALTRANS procedure, the final value of the 'design' stiffness by the AASHTO-83/ATC-6 procedure also would be the same as that from the CALTRANS procedure.

The numerical values the 'design' stiffness and the sample calculations have not been included in this paper for brevity; they are available elsewhere (Goel and Chopra, 1994).

Evaluation of Current Procedures for Estimating Abutment Stiffness

Compared in Figure 7a are the 'design' and 'actual' values of the stiffness normal to the east abutment. For each deformation level, the 'design' values are shown for the four possible failure modes of the abutments mentioned earlier; note that the figure shows only three lines because the stiffnesses for two of the four failure modes were almost identical. These results show that during the strong shaking phase, the 'design' values obtained by the CALTRANS procedure using 1 inch deformation are much larger than the 'actual' values estimated from the recorded motions. However, the 'design' values based on 2.4 inch deformation tend to be close to the 'actual' values. The peak deformation normal to the east abutment during the 1992 earthquake was about 1 inch in both positive and negative directions (Figure 3a). Thus, comparison of the 'design' value calculated for the actual earthquake induced deformation of 1 inch shows that the CALTRANS overestimates the normal stiffness by a factor of over two. During beginning and ending phases of the earthquake, when ground shaking is less intense, the actual deformation of the abutment is small and the CALTRANS procedure using either deformation level underestimates the stiffness.

Results for the transverse stiffness of the east abutment show that the 'design' value of the stiffness from the CALTRANS procedure for either deformation level may be significantly smaller than the 'actual' values during the earthquake (Figure 7b). This difference can be explained by noting that the earthquake-induced deformations were significantly smaller along the east abutment (Figure 3b) compared to those assumed by the CALTRANS procedure.

For the west abutment, the 'design' values by the CALTRANS procedure for the two deformation levels form the upper and lower bounds of the 'actual' stiffness values during the strong shaking phase (Figure 7c). Since the deformation of this abutment during the earthquake ranged between 1 inch and 2.4 inch (Figure 3c), the CALTRANS procedure leads to a good estimate of the abutment stiffness in the transverse direction. The CALTRANS procedure using either deformation level may underestimate the stiffness during the less intense motions near the end of the shaking because the deformation of the abutment is small.

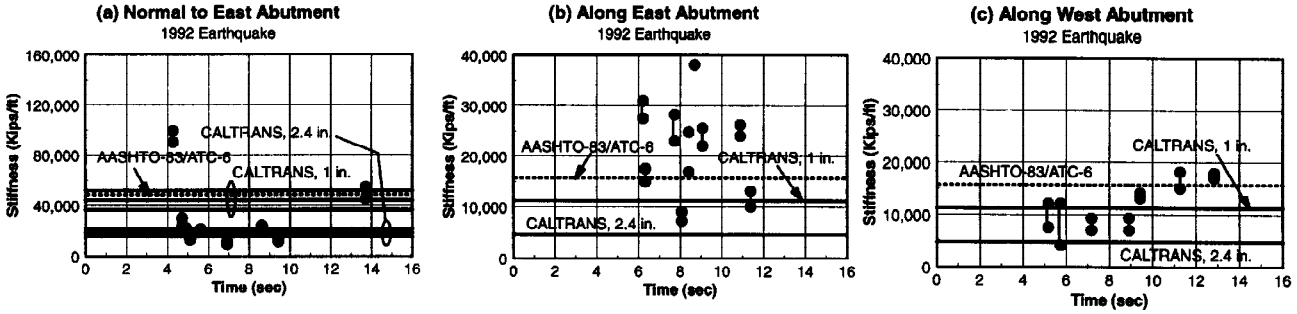

Figure 7. Comparison of 'design' and 'actual' values of abutment stiffness.

The above observations regarding the CALTRANS design value of abutment stiffness also apply to the final value of stiffness from the AASHTO-83/ATC-6 procedure. However, the AASHTO-83/ATC-6 procedure gives initial estimates of the stiffness normal to the east abutment and stiffness along the west abutment that are larger than the 'actual' stiffness during the strong shaking phase of the earthquake

(Figure 7). During the build-up phase and towards the end of the earthquake, however, the initial estimate may be reasonable. The initial estimate of the stiffness along the east abutment is larger than the 'actual' value because the deformations of this abutment are small during the earthquake.

CONCLUSIONS

In this investigation, the stiffness values of the abutment-soil systems at the US 101/Painter Street Overpass are determined from the ground and structural motions recorded during earthquakes using a simple equilibrium-based approach without finite-element modeling of the structure or of the abutment-soil systems. The values determined in this manner, which include the effects of soil-structure interaction and of nonlinear behavior of the soil, indicate that the abutment stiffness varies with time decreasing significantly as the abutment deformation increases.

Evaluation of the current design procedures indicates that the CALTRANS procedure leads to a good estimate of the abutment stiffness in the direction along the abutment (transverse to the road deck) provided the deformation assumed in computing the stiffness is close to the actual deformation during the earthquake. However, this procedure may overestimate the stiffness normal to the abutment (along the road deck) by a factor of over two indicating that the assumed value of 7.7 ksf for the ultimate passive resistance of the soil, which is used in the CALTRANS procedure, may be too high. The AASHTO-83/ATC-6 procedure gives an initial estimate of abutment stiffness that is too large in both directions. Since the abutment capacities by the AASHTO-83/ATC-6 procedure are identical to those by the CALTRANS procedure, both procedures give identical values for the final stiffness.

ACKNOWLEDGMENTS

This investigation was funded jointly by the Strong Motion Instrumentation Program, California Division of Mines and Geology and the California Department of Transportation. This support is gratefully acknowledged. Also acknowledged is the assistance provided by Bob Darragh, Moh-Jiann Huang, Praveen Malhotra, and Anthony Shakal in obtaining structural plans and earthquake records, and by Pat Hipley in implementing the CALTRANS procedure to calculate abutment stiffnesses.

REFERENCES

AASHTO-83. (1988). *Guide Specifications for Seismic Design of Highway Bridges,* American Association of State Highway and Transportation Officials, Washington, D.C.

ATC-6. (1981). *Seismic Design Guidelines for Highway Bridges*, Applied Technology Council, Berkeley, CA, October.

CALTRANS. (1988). *Memo to Designers 5-1,* California Department of Transportation, Division of Structures, Sacramento, CA, September.

CALTRANS. (1989). *Bridge Design Aids 14-1*, California Department of Transportation, Sacramento, CA, October.

Goel, R. K. and Chopra, A. K. (1994*). Seismic Response Study of US 101/Painter Street Overpass Using Strong Motion Records*, In Print, CSMIP Data Utilization Report, California Department of Conservation, Division of Mines and Geology, Office of Strong Motion Studies, December.

Lam, I. P. and Martin, G. R. (1986). *Seismic Design of Highway Bridge Foundations Volume II: Design Procedures and Guidelines*, Report No. FHWA/RD-86/102, Earth Technology Corporation, Long Beach, CA, June.